Phys Chem Minerals (1997) 24: 423–431

ORIGINAL PAPER

A. Takada · C.R.A. Catlow · G.D. Price
C.L. Hayward

Periodic ab initio Hartree-Fock study of trigonal and orthorhombic phases of boric oxides

Received July 21, 1994/Revised, accepted October 8, 1996

Abstract The structure and electronic properties of trigonal and orthorhombic boric oxide (B_2O_3) are studied using periodic ab initio Hartree-Fock method. The optimised structural parameters for two B_2O_3 polymorphs are in good agreement with experimental data. The analyses of their electronic structures provide insights into the chemical nature of the B–O bond and the way in which it changes with the coordination number around boron and oxygen. Our quantum-chemical study suggests that the orthorhombic form is more ionic than the trigonal form and that the coordination number of boron around oxygen plays a more dominant role than that of oxygen around boron in B_2O_3 crystals.

Introduction

Quantum mechanical studies have had a major impact on our understanding of bonding and cohesion in minerals (Tossell and Vaughan 1992). The present paper concerns their application to boric oxide crystals. Previously there have been several sets of cluster calculations, which have been used not only to discuss the π electron system and the basicity of borates, but which have also succeeded in reproducing bond lengths and bond angles in the crystalline state (Coulson 1964; Coulson and Dingle 1968; Snyder et al. 1976; Snyder 1978; Gupta and Tossell 1981; Gupta and Tossell 1983; Zhang et al. 1985; Uchida et al. 1985, 1986). However, such simulations have generally neglected crystal field effects, which almost certainly have a significant influence on bonding in polar solids. In companion studies we have investigated the structural transformation between B_2O_3 polymorphs by employing total-energy pseudopotential technique (Takada et al. 1995a); and have also modelled the crystalline phases and the vitreous structure by employing atomistic simulation techniques (Takada et al. 1995b, 1995c). In this paper we present the first results of Hartree-Fock calculations on B_2O_3 in the crystalline state, using periodic ab-initio methods. The differences between the electronic structures of the two B_2O_3 polymorphs are discussed; and we show that the changes in electronic structures associated with the coordination number of boron around oxygen are more significant than these related to that of oxygen around boron in B_2O_3 crystals.

Akira Takada (✉)
Fundamental Research Laboratory, Asahi Glass Co., Ltd.,
1150 Hazawa-cho, Yokohama 221, Japan

Akira Takada · C.R.A. Catlow
Davy Faraday Research Laboratory,
Royal Institution of Great Britain, 21 Albemarle Street,
London, W1X 4BS, U.K.

G.D. Price · C.L. Hayward[1]
Research School of Geological and Geophysical Sciences,
Birkbeck College and University College London,
Gower Street, London, W1E 6BT, U.K.

Present address:
[1] Department of Mineralogy, The Natural History Museum,
Cromwell Road, London, SW7 5BD, U.K.

Theoretical method

In order to perform the quantum chemical calculations, we used the periodic ab-initio Hartree-Fock code CRYSTAL-92 (Pisani et al. 1988; Dovesi et al. 1988). The program uses basis sets constructed from atomic orbitals (AO), similar to the approach used in standard molecular orbital programs (for example, GAUSSIAN, GAMESS, HONDO, MOPAC, AMPAC), but in the context of wave functions which satisfy the Bloch theorem. In addition, calculated properties, such as electron charge density maps and Mulliken charges, can be analysed using chemical concepts. The details of the theory are described in the monograph of Pisani et al. (1988). In the following section, we discuss some of the computational assumptions and restrictions necessary when applying the method to model B_2O_3 crystals.

Selection of a model

As periodic systems are being studied, CRYSTAL-92 as noted uses Bloch functions, $\phi_\mu(k)$, constructed from local functions, $\chi_\mu(r)$:

$$\phi_\mu(k; r)=\sum^g \chi_\mu(r-g) \exp(ik \cdot g) \quad (1)$$

The "generating" functions, χ_μ, are centred at the atomic nuclei and are expressed as a linear combination of Gaussian-type atomic orbitals (GTOs), as in molecular quantum chemical studies. Generally speaking, the larger the number of GTOs which are employed, the more accurate the calculated result within the Hartree-Fock (HF) limit. However, in contrast to the calculations on molecules, diffuse Gaussian orbitals (exponent of the order of 0.2 a.u. or less) play a crucial role in crystalline-state calculations and cause two problems (Pisani et al. 1988).

First we note that the number of integrals to be calculated explicitly increases dramatically with a decreasing exponent. Secondly we find that on decreasing the exponent the risks of pseudo-linear dependence increase rapidly, demanding higher precision in order to avoid "catastrophic" behaviour. However, such very diffuse AOs are much less important in three-dimensional densely packed crystals than in atoms and molecules, where they serve to describe the tails of the electronic distribution toward vacuum. Therefore, except for the case of the minimal basis set (STO-3 G), it is desirable when starting from the standard Pople basis set (Pople and Binkley 1975) to reoptimise the exponent of the outermost shell.

Secondly, in the present version of CRYSTAL-92, it is difficult simulate large systems, except at the minimal basis set level, because of restrictions related to the size of vectors and matrices. In order to overcome the limitation of system size in the all-electron calculations, pseudopotentials techniques have been developed (Hay and Wadt 1985 a, 1985 b, 1985 c; Durand and Barthelat 1975; Bouteiller et al. 1988). This technique was also tested for the B_2O_3 systems studied here.

As is well known, Hartree-Fock techniques do not include the effects of electron correlation which can only be represented using post Hartree-Fock techniques (Hehre et al. 1986). Correlation energies are, however, unlikely to influence the relative energies of the different structures discussed in this paper.

Optimisation of structure

Owing to the uncertainties in the experimentally determined crystal structures (for example, the positions of hydrogen atoms in boric acid crystals determined by X-ray techniques have errors of as much as 0.1 Å), it is desirable in simulations to relax not only unit cell dimensions but also internal coordinates, to achieve the minimum total energy. However, the automatic relaxation of cell dimensions or internal coordinates is not available in the present version of CRYSTAL, although manual, point by point, optimisation is possible. Therefore in the present study of B_2O_3 crystals, cell dimensions and internal coordinates were varied in a point by point manner and the variations in energy were tabulated in order to check the accuracy of the calculations. In contrast, the calculations on the other more complex borate crystals were carried out using fixed (experimentally determined) cell dimensions and atomic positions.

Mulliken population analysis

It is often useful to define the total electronic charge on a particular atom so that quantitative meaning may be given to such concepts as electron withdrawing or donating ability. The well-known Mulliken population analysis (Mulliken 1955) is often used for discussing the relative covalency and ionicity of materials, although some caution is required in the interpretation of the calculated populations. One problem concerns the definitions of 'ionicity' and 'covalency', as discussed by Catlow and Stoneham (1983). There is a considerable arbitrariness in these definitions and different charge partitioning schemes lead to different results. Another concerns the high sensitivity of the Mulliken charges to the basis-set (Hehre 1986). A third difficulty is that the charges are often not comparable with the effective charges obtained from experimental studies, and indeed the absolute value may have little meaning.

In this paper, we use only the *relative* order of the Mulliken atomic charges and overlap populations at different sites and among a variety of structures, in order to discuss relative degrees of 'ionicity' or 'covalency'.

Periodic ab-initio Hartree-Fock simulation of B_2O_3

Models for boron-oxygen bonding

The dominant oxidation state of boron is III and boron normally combines with oxygen to form three triangular-planar bonds by sp^2 orbital hybridization. The boron-

Table 1 B–O bond distances in borate minerals

Compound	B–O (Å) Triangular BO_3	B–O (Å) Tetrahedral BO_4	Ref.
Boron Trioxide			
B_2O_3-I	1.337, 1.366, 1.404 1.336, 1.384, 1.401		a
B_2O_3-II		1.373, 1.506, 1.507, 1.512	b
Potassium metaborate			
KBO_2	1.331 (in-ring) 1.398, 1.398 (out-of-ring)		c
Sodium metaborate			
$NaBO_2$	1.280 (in-ring) 1.433, 1.433 (out-of-ring)		d
Kotoito			
$Mg_3(BO_3)_2$	1.376, 1.392, 1.392		e
Magnesium Pyroborate			
$Mg_2B_2O_5$-II	1.35, 1.38, 1.38 1.33, 1.33, 1.37		f
Calcium Metaborate			
CaB_2O_4-I	1.326, 1.385, 1.401		g
Sinhalite			
$AlMgBO_4$		1.442, 1.483, 1.483, 1.586	h
Orthoboric acid			
$B(OH)_3$	1.356, 1.365, 1.365 1.353, 1.359, 1.365		i
Metaboric acid			
HBO_2-I			k
	1.345, 1.371, 1.386 1.356, 1.366, 1.378		
		1.433, 1.451, 1.452, 1.553	
HBO_2-II			l
		1.436, 1.465, 1.482, 1.505	
HBO_2-III			m
	1.373, 1.377, 1.391, 1.353, 1.372, 1.372 (in-ring) 1.351, 1.367, 1.347 (out-of-ring)		

Reference: (a) Gurr et al. 1970; (b) Prewitt and Shannon 1968; (c) Schneider and Carpenter 1970; (d) Marezio et al. 1963 b; (e) Effenberger and Pertlik 1984; (f) Takeuchi 1952; (g) Marezio et al. 1963 a; (h) Hayward 1993; (i) Zachariasen 1954; (j) Zachariasen 1963 a; (k) Zachariasen 1963 b; (l) Peters and Milberg 1964

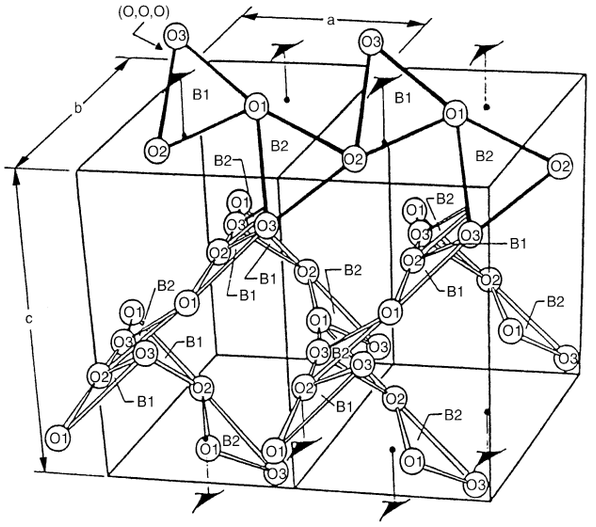

Fig. 1 The B_2O_3-I structure (Gurr et al. 1970)

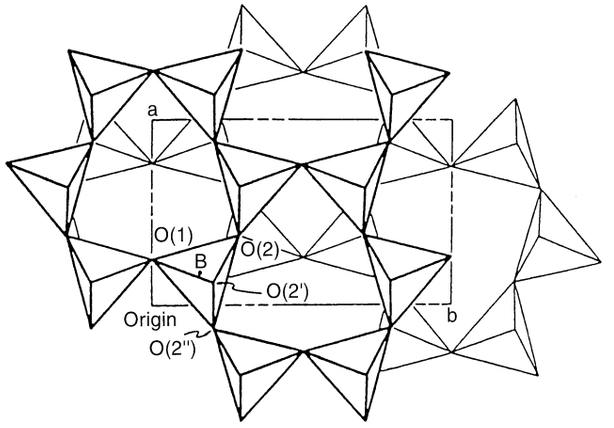

Fig. 2 The B_2O_3-II structure (Prewitt and Shannon 1968)

Table 2 Reoptimised exponents of outer shell for B_2O_3-I and B_2O_3-II

Basis set	Boron	Oxygen
3-21 G	0.15	0.40
6-21 G	0.12	0.40
PS 31 G	0.21	0.30

oxygen radius ratio is 0.20 and from spatial considerations alone, boron would be expected to occur in three- or four-fold coordination. The measured B–O bond distances in trigonal borates range from 1.28 to 1.44 Å and the mean is 1.37 Å. The mean tetrahedral bond length is 1.48 Å and the individual values vary from 1.42 to 1.54 Å. For refined structures having an experimental error of $\leq$0.05 Å, the difference between trigonal and tetrahedral bond lengths of 0.1 Å is significant (Ross and Edwards 1967).

The simple theoretical estimates of the trigonal B–O bond length, corresponding to the "single" covalent B–O bond distance, give a value of slightly less than 1.43 Å (Pauling 1960); its discrepancy with the measured lengths has been attributed to the presence of 20% double bond character. The measured B–O bond distances in some borate crystals are shown in Table 1.

Boron trioxide crystal structures

Crystals of boron trioxide do not exist naturally. Two different crystal phases have been synthesised and their structures determined (Figs. 1 and 2). All boron atoms in B_2O_3-I are in planar trigonal configurations consisting of ribbons of interconnected BO_3 triangles (Strong and Kaplow 1968; Gurr et al. 1970). The other crystalline polymorph B_2O_3-II comprises a network of corner-linked BO_4 tetrahedra (Prewitt and Shannon 1968).

Basis set effects

The basis set plays a crucial role in the description of crystalline orbitals. Starting from the standard Pople ba-

Table 3 Mulliken gross atomic charges and total energies for B_2O_3-I and B_2O_3-II

B_2O_3-I						
basis set	B(1)	B(2)	O(1)	O(2)	O(3)	E(a.u./B_2O_3)
boron/oxygen						
STO-3 G/3 G	+0.664	+0.661	−0.439	−0.435	−0.451	−270.6795
3-21 G/3-21 G	+1.048	+1.046	−0.688	−0.685	−0.721	−272.8511
6-21 G/6-21 G	+1.010	+1.005	−0.661	−0.660	−0.694	−273.9886
PS 31 G/PS 31 G	+1.404	+1.405	−0.925	−0.925	−0.959	–
B_2O_3-II						
basis set	B(1)		O(1)	O(2)		E(a.u./B_2O_3)
boron/oxygen						
STO-3 G/3 G	+0.659		−0.488	−0.415		−270.7587
3-21 G/3-21 G	+1.164		−0.708	−0.810		−272.8709
6-21 G/6-21 G	+1.128		−0.677	−0.790		−274.0111
PS 31 G/PS 31 G	+1.569		−0.947	−1.095		–

Table 4 Interatomic distances and interbond angles for B_2O_3-I and B_2O_3-II (Gurr et al. 1970; Prewitt and Shannon 1968)

B_2O_3-I	Distances (Å)	B_2O_3-II	Distances (Å)
B(1)–O(1)	1.404	B(1)–O(1)	1.373
–O(2)	1.366	–O(2)	1.507
–O(3)	1.337	–O(2′)	1.506
B(2)–O(1)	1.336	–O(2″)	1.512
–O(2′)	1.400	O(1)–O(2)	2.364
–O(3′)	1.384	–O(2′)	2.440
O(1)–O(2)	2.387, 2.388	–O(2″)	2.409
O(2)–O(3)	2.409, 2.333	O(2)–O(2′)	2.428
O(3)–O(1)	2.309, 2.408	–O(2″)	2.394
B(1)–B(2)	2.489, 2.489, 2.498	O(2′)–O(2″)	2.388
		B(1)–B(1′)	2.569
		–B(1″)	2.664
		–B(1‴)	2.664
		–B(1⁗)	2.592
Angles (deg)			
O(1)–B(1)–O(2)	119.0	O(1)–B(1)–O(2)	110.2
–O(3)	114.7	–O(2′)	115.8
O(2)–B(1)–O(3)	126.1	–O(2″)	113.1
O(1)–B(2)–O(2)	121.5	O(2)–B(1)–O(2′)	107.4
–O(3)	124.6	–O(2″)	104.9
O(2)–B(2)–O(3)	113.8	O(2′)–B–O(2″)	104.7
B(1)–O(1)–B(2)	130.5	B(1)–O(1)–B(1′)	138.6
–O(2)–B(2)	128.3	–O(2)–B(1″)	123.8
–O(3)–B(2)	133.4	–O(2″)–B(1‴)	123.8
		–O(2′)–B(1⁗)	118.7

Table 5 Potential energies with different lattice parameters for B_2O_3-I and B_2O_3-II. (@ indicate the minimum point)

	B_2O_3-I ΔE (a.u./B_2O_3)	B_2O_3-II ΔE (a.u./B_2O_3)
1) $v/v_0)^{1/3}$		
1.08	+0.05575	
1.06	+0.03150	
1.04	+0.01348	
1.02	+0.00261	
1.01	+0.00021	−0.00021
1.005	−0.00019 @	−0.00044 @
1.0	0	0
0.995	+0.00077	+0.00100
0.99	+0.00210	+0.00273
0.98	+0.00661	
0.96	+0.02299	
2) a/a_0	(a_0=4.339)	(a_0=7.842)
1.02	+0.00136	−0.00066
1.01	+0.00002	−0.00072 @
1.0	0 @	0
0.99	+0.00128	+0.00154
0.98		+0.00395
3) b/b_0	(b_0=4.339)	(b_0=4.636)
1.04		+0.01281
1.02		+0.00050
1.01		−0.00002 @
1.0		0
0.99		+0.00052
0.98		+0.00158
4) c/c_0	(c_0=8.340)	(c_0=4.150)
1.03	+0.00022	
1.02	+0.00013	+0.00136
1.01	−0.00020 @	+0.00002
1.0	0	0 @
0.99		+0.00128
0.98	+0.00119	

sis sets, the exponents of the outer shell are reoptimised. The reoptimised exponents and the Mulliken charges are compared in Tables 2 and 3.

Minimal basis set

As is generally recognised, the Mulliken charges obtained employing STO-3G tend to be smaller than with other basis sets (Hehre 1986). The more important problem is that the STO-3G result for B_2O_3-II is not consistent with the results for the other basis sets. The Mulliken charge on O(1) in B_2O_3-II is not only larger than the average of those on the oxygen atoms in B_2O_3-I, but also that on O(2) in B_2O_3-II. O(1) is two-fold coordinated by boron as well as the oxygen atoms in B_2O_3-I, while O(2) has three-fold coordination (Figs. 1 and 2). The two charge distributions are expected to be different, which is difficult to achieve using a minimal basis set. Therefore, inaccuracies are expected when a minimal basis set is applied to three-fold coordinated oxygen or four-fold coordinated boron.

Split-valence and polarization function

As even B_2O_3 crystals represent a large system, basis sets better than 6-21G, such as 8-51G, are not possible in the present version of CRYSTAL. For both polymorphs, the 6-21G basis set may be assumed to be satisfactory, as Dovesi et al. (1987) and Nada et al. (1990) suggested for SiO_2. The 3-21G basis set gives almost the same result as that for 6-21G.

Pseudopotentials

All electron calculations restrict the feasible system size. In order to overcome this problem, several types of pseudopotentials have been developed. In these pseudopotential techniques the role of core electrons is substituted by the effective core potentials and only the orbitals of valence electrons are calculated. Here only one available set, PS-31G (Bouteiller 1988), is tested. The orginal PS-31G sets were optimised for atoms and tested only on small molecules. Therefore, the exponents of the outermost shel were reoptimised for the periodic structures. The Mulliken charges reported in Table 3 are larger than those calculated with the all electron cases. This effect may be due to electron rich second shells, which are composed of three Gaussians, whereas the second shell in the outer all-electron calculations were composed of two Gaussians. The order of the charges seems reason-

Table 6 Potential energies with different internal coordinates for B_2O_3-I and B_2O_3-II

B_2O_3-I change of bond length	(Å)	ΔE (a.u./B_2O_3)			
		−10%	−5%	+5%	+10%
R(B–O(3))	1.337	+ 0.03754	+0.01590	+0.00166	+ 0.01341
R(B–O(1))	1.404	+ 0.02061	+0.00318	+0.00823	+ 0.02614
R(B–O(2))	1.366	+ 0.02740	+0.00685	+0.01691	+ 0.00406
change of bond angle	(deg)				
		−10°	−5°	+5°	+10°
∠O(1)–B–O(3)	114.8			+0.00711	+ 0.02535
∠O(2)–B–O(3)	126.1	+ 0.02398	+0.00326		
∠O(1)–B–O(3)	114.8			+0.00702	+ 0.02985
∠O(2)–B–O(1)	119.0	+ 0.05140	+0.01452		
∠O(2)–B–O(3)	126.1			+0.00669	+ 0.03270
∠O(2)–B–O(1)	119.0	+ 0.01016	+0.03480		
B_2O_3-II change of bond length	(Å)	ΔE (a.u./B_2O_3)			
		−10%	−5%	+5%	+10%
R(B–O(1))	1.373	+ 0.00111			− 0.00003
R(B–O(2))	1.507	+ 0.01001	+0.00814		
change of bond angle	(deg)				
		−10°	−5°	+5°	+10°
∠O(2)–B–O(2)′′	104.9		+0.00769		
∠O(2)–B–O(1)	110.2		+0.01064		

able, and indeed the results show that the pseudopotential technique is promising. These pseudopotentials will be a powerful aid for calculations on larger systems.

Geometry optimisation

In order to check the accuracy of our calculations, unit cell dimensions, bond lengths and bond angles were optimised using the 3-21G basis set. The interatomic distances and interbond angles are reported in Table 4, while the calculated energies are summarised in Table 5. The errors in the unit cell volume are 1.5% for B_2O_3-I and 1.5% for B_2O_3-II. The errors in the lattice parameters are ∼1% for both crystal structures. The atomic parameters were also varied in a point by point manner using the 3-21G basis set. The calculated results are shown in Table 6. For the B–O bond lengths, the error in the B–O(1) bond (the shortest B–O bond) of B_2O_3-II is appreciable (∼10%) but all the other errors are less than 5%; all the errors in O–B–O bond angles are also within 5%. Despite these appreciable discrepancies, the level of agreement of these calculations with experiment is acceptable for our present purposes. In the following sections all the results refer to the 3-21G basis set.

Electronic structure

In this section we calculate the band structures, the densities of states (DOSs), the overlap populations of B_2O_3-I and B_2O_3-II crystals. Then we discuss the differences between the electronic structures of the two phases.

Band structure and the density of states

The band structures for the two phases are shown in Fig. 3. The zero of the energy is taken at the edge of the valence band and only occupied bands are plotted. The total densities of state (DOSs) and the projected densities of states (PDOSs) are shown in Figs. 4 and 5. Top flat parts of their band structures are composed of non-bonding oxygen 2*p* orbitals, as seen from the analysis of the PDOSs. The bands lying between −4 eV and −11 eV are assigned to bonding crystalline orbitals involving oxygen 2*p* and boron 2*p* orbitals. The bands around −25 eV are due to oxygen 2*s* orbitals with contributions from boron 2*s* and 2*p* orbitals. Therefore, both phases exhibit the typical electronic structure of ionic oxides (Dovesi et al. 1987; Orlando et al. 1992).

Now we consider the differences between two phases. First the bandwidths of the p_O band are different: 11 eV for B_2O_3-I and 13 eV for B_2O_3-II. It is interesting to note that the PDOSs of two oxygen atoms (O1 for two-fold coordination and O2 for three-folded coordination) in B_2O_3-II have different patterns, but almost the same band widths. As Lichanot et al. (1991) discussed, the p_O band is strongly correlated to the oxygen-oxygen separation, Do-o, between the nearest oxygen atoms and, to a lesser extent, to their number. In this study, the average Do-o is 2.372 Å for B_2O_3-I and 2.404 Å for B_2O_3-II. B_2O_3-II has almost the same O–O distances although it has short and long B–O lengths as shown in Table 4. Therefore, the difference of the bandwidths can be attributed to the differences in Do-o. Furthermore, the difference can be explained in terms of the higher density and ionicity of B_2O_3-II: the Madelung field at the oxygen site is higher and there is a stronger interaction between the electron clouds of next neighbour oxygen atoms, as Nada et al.

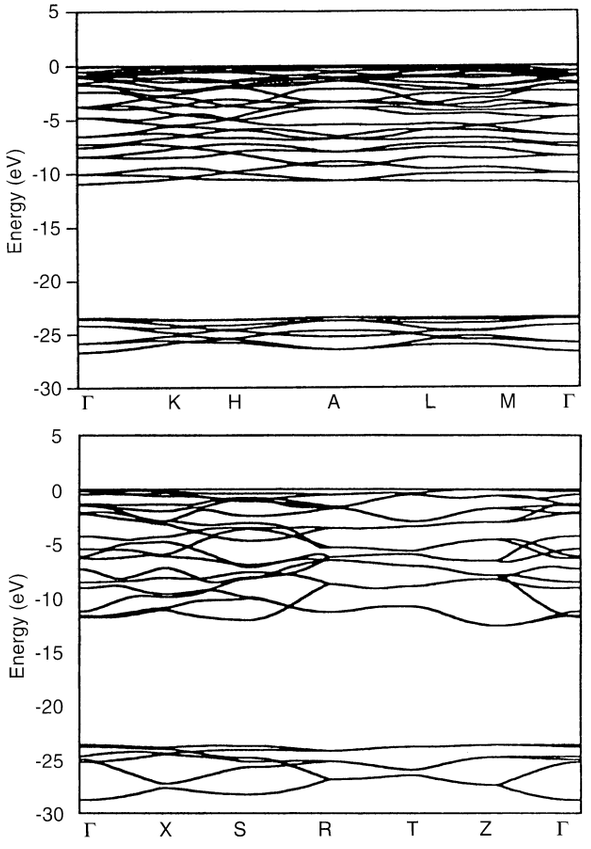

Fig. 3 Band structures for B_2O_3-I (top) and B_2O_3-II (bottom)

(1990) discussed for the difference between α-quartz and stishovite.

Next there is a distinctive difference in the height of the PDOS peak of oxygen near the zero level: the peak of $2p$ O 2 in B_2O_3-II ($\sim$24 in arbitrary units) is much lower than those of $2p$ O in B_2O_3-I ($>$40) and $2p$ O 1 in B_2O_3-II ($>$40). These peaks comprise a predominant contribution from the oxygen lone-pair ($2p$ non-bonding orbitals) with little contributions from boron $2s$ and $2p$ orbitals. Therefore, it is reasonable to propose that the three-fold coordinated oxygen atom (O 2 in B_2O_3-II) has much less marked lone-pair behaviour than is the case for the two-fold coordinated oxygen atoms (i.e. any O in B_2O_3-I and O 1 in B_2O_3-II). There is also a sharper peak for the $2s$ of O 1 in B_2O_3-II than for those of any O in B_2O_3-I and O 2 in B_2O_3-II, which can be attributed to the crystallographically higher symmetry of the position of O 1 oxygen.

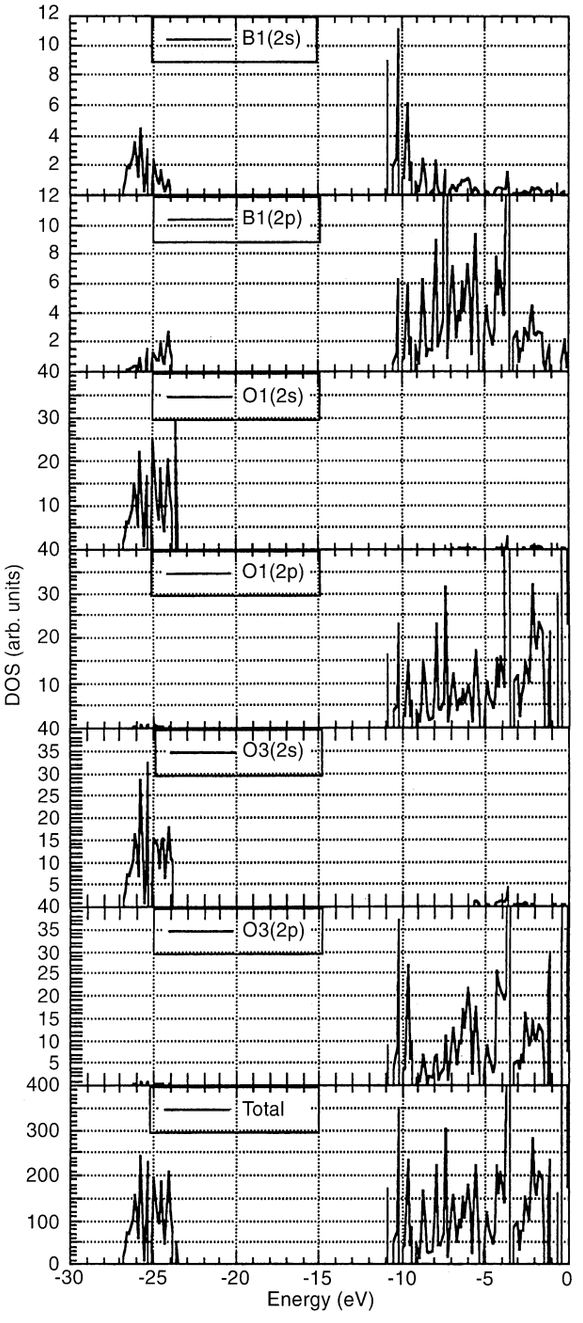

Fig. 4 Total and Projected Density of States of B_2O_3-I

Mulliken population analysis

The Mulliken population analysis is shown in Tables 3 and 7. Gross atomic charges in Table 3 and both the B–B and O–O net atomic populations in Table 7 show that more charge is transfered from boron atoms to oxygen atoms in B_2O_3-II than in B_2O_3-I; that is, B_2O_3-II is more ionic than B_2O_3-I. It is interesting to note that the O(1)–O(1) (the two-fold coordinated oxygen) net atomic population in B_2O_3-II (8.102) is closer to the O–O (the two-fold coordinated oxygen) populations in B_2O_3-I (average 8.109) than the O(2)–O(2) (the three-fold coordinated oxygen) population in B_2O_3-II (8.334). Moreover, the B(1)–O(1) overlap populations in B_2O_3-II (0.358) is closer to the B–O overlap populations in B_2O_3-I (average 0.320) than the B(1)–O(2) overlap populations in B_2O_3-

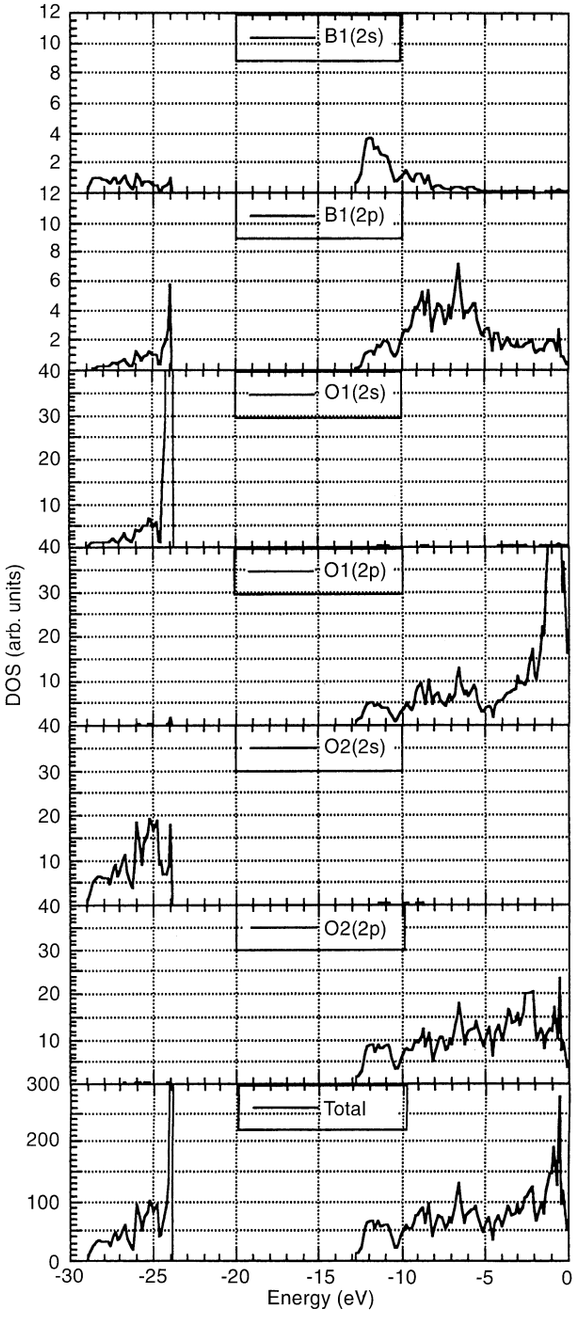

Fig. 5 Total and Projected Density of States of B_2O_3-II

II (average 0.207). These results show that the boron-oxygen bonding is more affected by coordination number around oxygen than by that around boron. A larger boron-oxygen overlap population between boron and the two-fold coordinated oxygen atom suggests the existence of stronger covalent bonds than that between boron and the three-fold coordinated oxygen atom.

Table 7 Mulliken population analysis for B_2O_3-I and B_2O_3-II. Overlap populations are condensed to atoms for first neighbours

B_2O_3-I		
	Distances (Å)	net atomic or overlap populations
B(1)–B(1)	0.0	2.981
B(1)–O(1)	1.404	0.306
–O(2)	1.366	0.333
–O(3)	1.337	0.316
B(2)–B(2)	0.0	2.984
B(2)–O(1)	1.336	0.342
–O(2′)	1.400	0.318
–O(3′)	1.384	0.307
O(1)–O(1)	0.0	8.095
O(2)–O(2)	0.0	8.092
O(3)–O(1)	0.0	8.140
B_2O_3-II		
	Distances (Å)	net atomic or overlap populations
B(1)–B(1)	0.0	2.913
B(1)–O(1)	1.373	0.358
–O(2)	1.507	0.207
–O(2′)	1.506	0.213
–O(2″)	1.512	0.200
O(1)–O(1)	0.0	8.102
O(2)–O(2)	0.0	8.334

Discussion

We first note that the average experimental B–O bond distance of 1.372 Å in B_2O_3-I agrees well with the length assumed by Zachariasen (1963b) for a bond of 'strength' 1.0 (1.365 Å), and also with a value of 1.37 ± 0.02 Å which was quoted as the mean B–O distance for three-coordinated boron by Waugh (1968). The near planar shape of the BO_3 triangle and the small Mulliken atomic charges emphasise the partially covalent character of the bonding, while the larger Mulliken atomic charge of O(3) as well as the larger overlap populations of O(3)–O(3) indicates the presence of some ionic character. The latter ionic character is a possible cause of the distortion of the BO_3 triangle.

In discussing the charge of O(3), Gurr et al. (1970) distinguished O(3) from the other oxygen atoms by suggesting it had an effective 'higher coordination' as a result of the linking of adjacent ribbons, although strictly O(3) is still two-fold coordinated. Madelung potentials are calculated (using formal charges) as −66.42, −65.49 and −67.18 (eV) for O(1), O(2) and O(3). The larger value for O(3) is in agreement with Gurr's interpretation and is the obvious explanation for the large Mulliken atomic charge of O(3).

If we now consider B_2O_3-II, the average B–O distance is 1.475 Å, exactly that proposed by Zachariasen (1963b) as an average tetrahedral B–O distance. However, the tetrahedron is very distorted, with one short B–O(1) distance of 1.373 Å and three long B–O(2) distances of 1.507, 1.506 and 1.512 Å. O(1) is two-fold coordinated, while O(2) is three-fold coordinated.

Prewitt and Shannon (1968) calculated electrostatic bond strengths in B_2O_3-II using Zachariasen's table of bond strength versus B–O bond length (Zachariasen 1963b). The calculated net bond strength is 3.01 around B, 1.96 around O(1), and 2.03 around O(2). They concluded that the distortions are necessary to balance the electrostatic charge in the crystal.

When the Mulliken atomic charges of O(1) and O(2) in B_2O_3-II (except in the case of minimal basis set) are compared, the charge of O(1) is found to be much smaller than that of O(2). It is also interesting to note that the O–O distances of the four oxygens (one O(1) and three O(2)) are almost same, although the B–O(1) bond length is shorter than the others. This means that the tetrahedral arrangement of the four oxygens is not very distorted; but rather within the tetrahedron, B is displaced towards O(1). It seems reasonable therefore to assume that the difference in coordination number around oxygen chiefly changes the B–O bond strengths rather than the O–O repulsion. To check whether the distortion can be explained in terms of charge transfer between boron and oxygen atoms, we performed a lattice energy minimization using a simple rigid ion model (Takada et al. 1995b). Such a model, which assigns the Mulliken charge to each atom, cannot, however, explain the short B–O(1) bond length; indeed if the charge of O(1) is set to be smaller than O(2), the B–O(1) distance becomes longer, owing to the smaller attraction between B and O(1). However, the other interpretation namely that B–B repulsion shortens the B–O bond length is also possible. But the comparisons of the results of perfect lattice relaxation calculations, using several different sets of empirically fitted B–O Morse terms and B–B Buckingham terms, show that the changes in the B–O Morse term (i.e. the B–O bond strength) can more effectively reproduce the detailed structure than can be achieved by changing the B–B repulsive term (Takada et al. 1995b).

As Johnson et al. (1982) pointed out, one short bond B–O(1) distance in B_2O_3-II (1.373 Å) is close to the average B–O distance in B_2O_3-I (1.372 Å) and in B_2O_3 glass (1.37 Å). The calculated Mulliken atomic charges also show that the charge of O(1) in B_2O_3-II (−0.708 with STO 3-21G) is close to the average oxygen charge in B_2O_3-I (−0.698 with STO 3-21G). Moreover, the O–O and B–O overlap populations have the same trend as explained in the previous section. Thus regarding the two B_2O_3 crystal structures, it is interesting to note that the coordination number of boron around oxygen seems to affect the B–O distance much more than the coordination of oxygen around boron.

To summarise, the calculated Mulliken charges and PDOSs confirm that B_2O_3-II is more ionic than B_2O_3-I, which is compatible with the idea that a high-pressure or high-coordination structure generally has higher ionicity. The short B–O bond length in B_2O_3-II can be explained in two related ways: first, Pauling's electrostatic valence sum rule empirically suggests that the two-fold coordinated oxygen has a stronger electrostatic bond than that of three-fold coordinated oxygen; secondly, the larger B–O overlap population between boron and the two-fold coordinated oxygen atom suggests that the character of covalency strengthens the B–O bond.

Acknowledgements We gratefully acknowledge useful discussions with Drs. R. Nada, S. Hill and J.D. Gale

References

Bouteiller Y, Mijoule C, Nizam M, Barthelat JC, Daudey JP, Pelissier M, Silvi B (1988) Extended gaussian-type valence basis sets for calculations involving non-empirical core pseudopotentials. Mol Phys 65: 295–312

Catlow CRA, Stoneham AM (1983) Ionicity in solids. J Phys C 16: 4321–4338

Coulson CA (1964) The B–O bond lengths in orthorhombic metaboric acid. Acta Crystallogr 17: 1086

Coulson CA, Dingle TW (1968) The B–O bond lengths in boron-oxygen compounds. Acta Crystallogr B 24: 153–155

Dovesi R, Pisani C, Roetti C, Silvi B (1987) The electronic structure of α-quartz: A periodic Hartree-Fock calculation. J Chem Phys 86: 6967–6971

Dovesi R, Pisani C, Roetti C, Causa M, Saunders VR (1988) Quantum Chemistry Program Exchange. Publication 577, University of Indiana

Durand PH, Barthelat JC (1975) Theoretical method to determine atomic pseudopotentials for electronic structure calculations of molecules and solids. Theor Chim Acta 38: 283–302

Effenberger H, Pertlik F (1984) Verfeinerung der Kristallstrukturen der isotypen Verbindungen $M_3(BO_3)_2$ mit M=Mg, Co und Ni (Strukturtyp: Kotoit). Z Kristallogr 166: 129–140

Gupta A, Tossell JA (1981) A theoretical study of bond distances, x-ray spectra and electron density distributions in borate polyhedra. Phys Chem Minerals 7: 159–164

Gupta A, Tossell JA (1983) Quantum mechanical studies of distortions and polymerization of borate polyhedra. Am Mineral 68: 989–995

Gurr GE, Mongomery PW, Knutson CD, Gorres BT (1970) The crystal structure of trigonal diboron trioxide. Acta Crystallogr B 26: 906–915

Hay PJ, Wadt WR (1985a) Ab initio effective core potentials for molecular calculations. Potentials for the transition metal atoms Sc to Hg. J Chem Phys 82: 270–283

Hay PJ, Wadt WR (1985b) Ab initio effective core potentials for molecular calculations. Potentials for main group elements Na to Bi. J Chem Phys 82: 284–298

Hay PJ, Wadt WR (1985c) Ab initio effective core potentials for molecular calculations. Potentials for K to Au including the outermost core orbitals. J Chem Phys 82: 299–310

Hayward CL (1993) The vibrational spectroscopy of borate minerals. PhD Thesis, University College London

Hehre WJ, Radom L, Schleyer PvR, Pople JA (1986) Ab Initio Molecular Orbital Theory. John Wiley & Sons

Johnson PAV, Wright AC (1982) A neutron diffraction investigation of the structure of viteous boron trioxide. J Non-Cryst Solids 50: 281–311

Lichanot A, Gelize M, Larrieu C, Pisani C (1991) Hartree-Fock ab initio study of relaxation and electronic structure of lithium oxide slabs. J Phys Chem Solids 52: 1155–1164

Marezio M, Plettinger HA, Zachariasen WH (1963a) Refinement of the calcium metaborate structure. Acta Crystallogr 16: 390–392

Marezio M, Plettinger HA, Zachariasen WH (1963b) The bond lengths in the sodium metaborate structure. Acta Crystallogr 16: 594–595

Mulliken RS (1955a) Electronic population analysis on LCAO-MO molecular wave functions. I. J Chem Phys 23: 1833–1840

Mulliken RS (1955b) Electronic population analysis on LCAO-

MO molecular wave functions. II. Overlap populations, bond orders and covalent bond energies. J Chem Phys 23: 1841–1846
Mulliken RS (1955 c) Electronic population analysis on LCAO-MO molecular wave functions. III. Effects ofhybridization on overlap and gross AO populations. J Chem Phys 23: 2338–2342
Mulliken RS (1955 d) Electronic population analysis on LCAO-MO molecular wave functions. IV. Bonding and antibonding in LCAO and valence-bond theories. J Chem Phys 23: 2343–2346
Nada R, Catlow CRA, Dovesi R, Pisani C (1990) An ab-initio Hartree-Fock study of α-quartz and stishovite. Phys Chem Minerals 17: 353–362
Orlando R, Pisani C, Roetti C, Stefanovich E (1992) Ab initio Hartree-Fock study of tetragonal and cubic phases of zirconium dioxide. Phys Rev B 45: 592–601
Pauling L (1960) The Nature of the Chemical Bond. 3rd Ed., Cornell University Press
Peters CR, Milberg ME (1964) The refined structure of orthorhombic metaboric acid. Acta Crystallogr 17: 229–234
Pisani C, Dovesi R, Roetti C (1988) Hartree-Fock Ab Initio Treatment of Crystalline Systems (Lecture Notes in Chemistry 48), Springer-Verlag
Pople JA, Binkley JS (1975) Correlation energies for AH_n molecules and cations. Mol Phys 29: 599–611
Prewitt CT, Shannon RD (1968) Crystal structure of a high-pressure form of B_2O_3. Acta Crystallogr B 24: 869–874
Ross VF, Edwards (1967) The structure chemistry of the borates. In: Muetterties EL (ed), The Chemistry of Boron and its Compounds. John Wiley & Sons, Chaper 3
Schneider W, Carpenter GB (1970) Bond lengths and thermal parameters of potassium metaborate $K_3B_3O_6$. Acta Crystallogr B 26: 1189–1191
Snyder LC (1978) Quantum chemical calculations to model borate glass electronic structure and properties. In: Pye LD, Frechett VD, Kreidl NJ (eds) Borate Glasses: Structure, Properties, Applications. Plenum, pp 151–165
Snyder LC, Peterson GE, Kurkjian CR (1976) Molecular orbital calculations of quadrupolar coupling of ^{11}B in molecular models of glasses. J Chem Phys 64: 1569–1573
Strong SL, Kaplow R (1968) The structure of crystalline B_2O_3. Acta Crystallogr B 24: 1032–1036
Takada A, Catlow CRA, Lin JS, Price GD, Lee MH, Milman V, Payne MC (1995 a) Ab initio total-energy pseudopotential calculations for polymorphic B_2O_3 crystals. Phys Rev B 51: 1447–1455
Takada A, Catlow CRA, Price GD (1995 b) Computer modelling of B_2O_3: part I. New interatomic potentials, crystalline phases and predicted polymorphs. J Phys C 7: 8659–8692
Takada A, Catlow CRA, Price GD (1995 c) Computer modelling of B_2O_3: part II. Molecular dynamics simulations of vitreous structures. J Phys C 7: 8693–8722
Takeuchi Y (1952) The crystal structure of magnesium pyroborate. Acta Crystallogr 5: 574–581
Tossell JA, Vaughan DJ (1992) Theoretical Geochemistry: Application of Quantum Mechanics in the Earth and Mineral Sciences. Oxford University Press
Uchida N, Maekawa T, Yokokawa T (1985) An application of MNDO calculation to borate polyhedra. J Non-Cryst Solids 74: 25–36
Uchida N, Maekawa T, Yokokawa T (1986) MNDO studies of basicity of borate glasses. J Non-Cryst Solids 85: 290–308
Waugh JLT (1968) Isopolyborates. In: Rich A, Davidson N (ed) Structural Chemistry and Molecular Biology. Freeman, pp 731–749
Zachariasen WH (1954) The precise structure of orthorhombic acid. Acta Crystallogr 7: 305–310
Zachariasen WH (1963 a) The crystal structure of cubic metaboric acid. Acta Crystallogr 16: 380–384
Zachariasen WH (1963 b) The crystal structure of monoclinic metaboric acid. Acta Crystallogr 16: 385–389
Zhang ZG, Boisen MB Jr., Finger LW, Gibbs GV (1985) Molecular mimicry of the geometry and charge density distribution of polyanions in borate minerals. Am Mineral 70: 1238–1247